

## Localized Synchronization in Two Coupled Nonidentical Semiconductor Lasers

A. Hohl,<sup>1</sup> A. Gavrielides,<sup>1</sup> T. Erneux,<sup>2</sup> and V. Kovanis<sup>1</sup>

<sup>1</sup>*Nonlinear Optics Group, Phillips Laboratory, 3550 Aberdeen Avenue SE, Kirtland AFB, New Mexico 87117-5776*

<sup>2</sup>*Université Libre de Bruxelles, Optique Nonlinéaire Théorique, Campus Plaine, C. P. 231, 1050 Bruxelles, Belgium*

(Received 6 January 1997)

The dynamics of two mutually coupled but nonidentical semiconductor lasers are studied experimentally, numerically, and analytically for weak coupling. The lasers have dissimilar relaxation oscillation frequencies and intensities, and their mutual coupling strength may be asymmetric. We find that the coupled lasers exhibit a form of localized synchronization characterized by low amplitude oscillations in one laser, but large oscillations in the second laser. [S0031-9007(97)03442-X]

PACS numbers: 42.65.Sf, 42.55.Px

Coupled arrays of semiconductor lasers are of great technological importance due to their potential application as high power coherent light sources [1]. A successful device will require quality synchronization between lasers. Traditionally, synchronization describes the phenomenon of frequency entrainment in a system of individual elements that have slightly different intrinsic frequencies but that lock to one common frequency as they are weakly coupled [2]. How weakly coupled oscillators synchronize is a common question for a variety of systems from coupled mechanical oscillators, populations of biological cells, pairs of neurons, and Josephson Junctions to chemical oscillators and lasers [3–7].

Synchronization in a set of coupled oscillators is typically modeled mathematically by considering units of identical oscillators with the same amplitude but slightly different frequencies that are symmetrically coupled [8]. Synchronization is found when the spread of the oscillating frequencies is not too large. In a physical setting, however, the individual oscillators can be quite dissimilar in amplitude as well as in oscillating frequency due to manufacturing constraints. Also, the coupling between the oscillators need not be symmetric. The possible forms of synchronization between quite different oscillators are much harder to predict theoretically. For laser arrays, this may depend on the particular laser system considered, such as solid state versus semiconductor lasers or evanescently coupled versus mutually coupled.

One new form of synchronization, *localized synchronization*, appears when one or more oscillators in a coupled array exhibit large amplitude oscillations whereas the remaining oscillators exhibit small oscillations. These spatially localized solutions are often called breathers and are currently intensively investigated [9]. In the context of two coupled oscillators localized synchronization means that one of the oscillators exhibits strong oscillations and the other one weak oscillations [10]. This kind of synchronization was recently analyzed theoretically in a system of two weakly coupled solid state lasers [11].

The response of two coupled lasers has been first studied for CO<sub>2</sub> [4] and Nd:YAG lasers [5,6]. In these systems instabilities arise through successive subharmonic reso-

nances [12]. In contrast, instabilities in coupled semiconductor lasers appear through Hopf bifurcations [7]. Synchronization in lasers was demonstrated experimentally in spatially coupled—but nearly identical—pump modulated Nd:YAG lasers for chaotic amplitude fluctuations [6]. It has been suggested theoretically that three evanescently coupled identical semiconductor lasers can exhibit synchronized chaotic amplitude fluctuations for a range of coupling strength [7]. Experimentally these predictions have yet to be verified.

In this Letter we demonstrate experimentally, numerically, and analytically that a system of two mutually coupled but nonidentical semiconductor lasers can exhibit a form of stable localized synchronization. Specifically, we investigate a system of two coupled semiconductor lasers where each laser is pumped at a different level. Thus they admit dissimilar free-running relaxation oscillating frequencies and intensities; in addition the coupling strength may be asymmetric. Surprisingly we find that the laser which is pumped at the lower level may entrain the laser that is pumped at a considerably higher level. Here synchronization means locking of the relaxation oscillation frequencies of the individual lasers. This is the first experimental demonstration of localized synchronization in a system of coupled nonidentical semiconductor lasers.

In our system we couple two semiconductor lasers by mutually injecting light from one into the other (Fig. 1). This configuration enables us in the experiment to independently control the coupling strength, the detuning between the optical frequencies of the lasers, and their individual pump levels. We deliberately keep the coupling

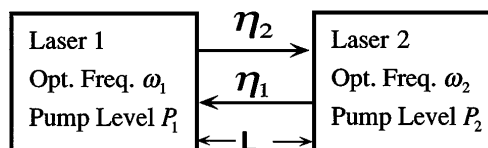


FIG. 1. Schematic of a system of two nonidentical semiconductor lasers mutually coupled at a distance  $L$  used to observe localized synchronization. We find that the laser which is pumped at a high level may be forced to entrain to the laser which is pumped at a significantly lower level.

strength weak in order to avoid the excitation of more than one external cavity mode [13,14]. We extract the underlying dynamics by observing the optical spectra [15] since the intensity fluctuations in coupled semiconductor lasers may take place at a subnanosecond time scale [16].

In the experiment we used two commercially available single-mode semiconductor lasers (Sharp LT015 lasing at 830 nm) and coupled them at a distance of  $L = 20$  cm. Two collimating lenses were used to mode-match the beams of the two lasers. The coupling strength was controlled by a set of three polarizers so that less than  $10^{-4}$  of the intensity of one laser was injected into the other. Symmetric mutual coupling, i.e.,  $\eta_1 = \eta_2$  (Fig. 1), was ensured by imaging the beam of laser 1 and the light of laser 2, which passed the polarizers and was reflected from the front facet of laser 1, on the same spot. The same procedure was repeated for the beam of laser 2 and the transmitted beam of laser 1. Through adjustments of the temperature, the lasers were tuned to the same optical frequency, but their pump levels were kept dissimilar. Laser 1 was pumped at 46% and laser 2 at 54% above threshold, resulting in output powers of 25.4 and 31.4 mW, and free-running relaxation oscillation frequencies of  $f_1 = 3.4$  GHz and  $f_2 = 4.0$  GHz. The optical spectrum was monitored with a scanning Fabry Perot interferometer which had a free spectral range of 2000 GHz (Newport SR-240C). The optical spectra confirmed that each of the lasers was lasing at only one single external cavity mode.

Figures 2(a) and 2(b) show the optical spectra of laser 1 and laser 2 with no coupling. The arrows show the location of the free-running relaxation oscillation frequencies  $f_1$  and  $f_2$ . As the two lasers are weakly coupled,  $f_1$  in laser 1 becomes undamped as indicated by strong relaxation oscillation sidebands at  $f_1$  and higher harmonics of  $f_1$  [Fig. 2(c)]. The spectrum of laser 2 [Fig. 2(d)] taken for the same coupling strength shows sidebands that are also located at  $f_1$  but that are considerably weaker. Thus the two coupled lasers exhibit a form of localized synchronization characterized by frequency  $f_1$ . Note that laser 2 is pumped at a high level, but is forced to oscillate at the relaxation oscillation frequency of laser 1 which is pumped at a lower level. We have also observed that laser 1 may be entrained to laser 2 at frequency  $f_2$  by slightly misaligning the collimating lenses and thereby introducing an asymmetry. However, the individual coupling strength for each laser could not be estimated with sufficient accuracy.

The system of these two mutually coupled semiconductor lasers can be modeled using single-mode semiconductor laser rate equations. Each laser is described by one equation for the normalized complex electric field,  $E$ , and one for the normalized carrier number above threshold,  $N$  [7]. The coupling is accounted for by adding a delayed electric field of laser 2,  $E_2(t - \tau)$ , with a real coupling efficiency of  $\eta_1$  to the equation for the complex electric field of laser 1 and vice versa [14]. Self-coupling caused by reflections from the front facet of one laser back into the other is neglected because it is of  $\mathcal{O}(\eta_m^2)$  small ( $m = 1, 2$ )

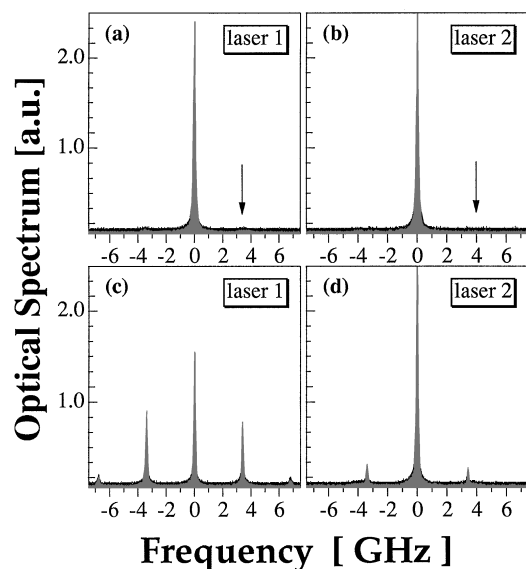


FIG. 2. Experimental optical spectra of the two lasers demonstrating localized synchronization. Arrows show the location of weak relaxation oscillation sidebands at  $f_1 = 3.4$  GHz (a) and at  $f_2 = 4.0$  GHz (b) for no coupling. The frequencies have been measured by expanding the vertical scale. With weak coupling (c) laser 1 exhibits strong undamped relaxation oscillation sidebands at  $f_1$  and (d) laser 2 exhibits weak sidebands also at  $f_1$ .

and is therefore much smaller than the cross coupling. The complete set of equation is given by:

$$E_1' = (1 + i\alpha)N_1E_1 + \eta_1E_2(t - \tau) + i\omega_1E_1, \quad (1)$$

$$E_2' = (1 + i\alpha)N_2E_2 + \eta_2E_1(t - \tau) + i\omega_2E_2, \quad (2)$$

$$TN_1' = P_1 - N_1 - (1 + 2N_1)|E_1|^2, \quad (3)$$

$$TN_2' = P_2 - N_2 - (1 + 2N_2)|E_2|^2. \quad (4)$$

Prime indicates a derivative with respect to time, where time is measured in units of the photon lifetime  $\tau_p$ ,  $\alpha$  is the linewidth enhancement factor,  $\omega_m$  denotes the normalized optical frequencies of each laser, and  $T$  is the ratio of the carrier lifetime  $\tau_s$  to  $\tau_p$ . The delay time  $\tau = L/c\tau_p$  corresponds to the time it takes for the light to travel the distance  $L$  from one laser to the other.  $P_m$  denotes the pumping above threshold for each laser.

We numerically integrated Eqs. (1)–(4) using typical parameters for the GaAlAs lasers used in the experiment:  $T = 700$ ,  $\tau = 476$  ( $L = 20$  cm),  $\alpha = 5$ ,  $\omega_1 = \omega_2$ , and  $\omega_m\tau = 2n\pi$ ,  $n$  integer. The lasers were pumped at 31.3% and 43.3% above threshold to match the relaxation oscillation frequencies of  $f_1$  and  $f_2$  in the experiment. Figures 3(a) and 3(b) show optical spectra computed for  $\eta_1 = 8.1 \times 10^{-4}$  and a ratio of  $C \equiv \eta_2/\eta_1 = 1.0$ . The optical spectrum of laser 1 shows strong undamped relaxation oscillation sidebands at  $f_1$  [Fig. 3(a)] and laser 2 also has sidebands at  $f_1$  but smaller in amplitude [Fig. 3(b)]. Thus laser 2 which is pumped at a higher level is entrained to the relaxation oscillation frequency

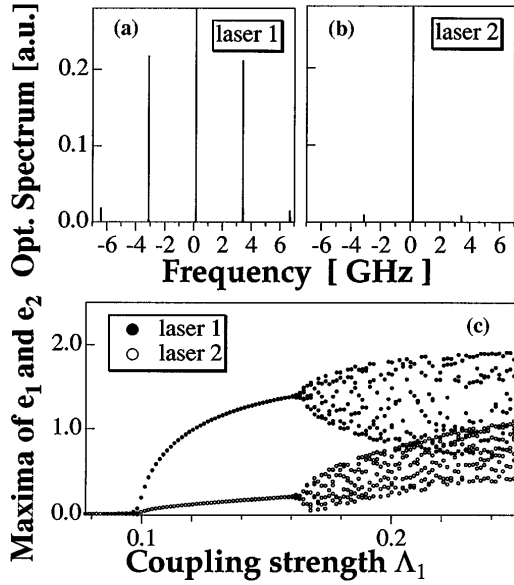


FIG. 3. Optical spectra of the two lasers computed from Eqs. (1)–(4) demonstrating localized synchronization ( $\tau_p = 1.4$  ps,  $\tau_s = 1$  ns,  $T = 700$ ,  $\tau = 476$ ,  $\alpha = 5$ ,  $P_1 = 0.313$ ,  $P_2 = 0.433$ ,  $\omega_1 = \omega_2$ ,  $\eta_1 = 8.1 \times 10^{-4}$ , and  $C = 1.0$ ). (a) Laser 1 shows strong sidebands at  $f_1$ . (b) Laser 2 shows weak sidebands at  $f_1$ . (c) Corresponding numerical bifurcation diagram depicting the maxima of the deviation from steady state  $e_1$  and  $e_2$ , where  $E_m = \sqrt{P_m}(1 + e_m/\alpha)\exp[i(\Phi_m + \omega_m t)]$ , versus the normalized coupling strength  $\Lambda_1 = \alpha\eta_1/\Omega$ . The lasers undergo a Hopf bifurcation into a limit cycle for  $\Lambda_1 = 0.1$  and quasiperiodicity appears for  $\Lambda_1 = 0.16$  as a frequency close to the external cavity frequency is excited.

of laser 1. As we change the coupling ratio to  $C > 1.4$ , we observe that laser 1 is entrained by laser 2 at  $f_2$  where laser 2's sidebands are much stronger than those of laser 1. We thus found numerically that each laser can exhibit localized synchronization at the relaxation oscillation frequency of the other laser, depending on the asymmetric coupling coefficient  $C$ . Systematic insight into the dynamical behavior of the system can be gained by computing a corresponding bifurcation diagram [Fig. 3(c)]. As the coupling strength is increased, the lasers undergo a bifurcation from steady state into a limit cycle for which both lasers oscillate at  $f_1$ , laser 1 strongly and laser 2 weakly. The limit cycle then bifurcates into a quasiperiodic state.

In order to understand the mechanism of localized synchronization analytically, we apply an asymptotic method that takes advantage of the two large parameters that are inherently present in a semiconductor laser, the ratio  $T$  and the linewidth enhancement factor  $\alpha$  [17]. We have verified numerically that the leading approximation is in good agreement with the solution of the full laser equations [Eqs. (1)–(4)] if  $T = 1000$  and  $\alpha = 10$ . For smaller values of  $\alpha$  we have found no qualitative changes in the bifurcation diagram (i.e., same bifurcation transitions). Introducing  $s = \Omega t$ , where  $\Omega = \sqrt{2P_1/T}$  is the free-running relaxation oscillation frequency of laser

1,  $E_m = \sqrt{P_m}(1 + e_m/\alpha)\exp[i(\Phi_m + \omega_m t)]$  and  $N = \Omega n_m/\alpha$  into Eqs. (1)–(4) and neglecting all  $\mathcal{O}(1/\alpha)$  correction terms, we obtain the following set of equations:

$$\Phi_1''' + \xi_1\Phi_1'' + \Phi_1' + r\Lambda_1\cos\psi_1 = 0, \quad (5)$$

$$\Phi_2''' + \xi_2\Phi_2'' + r^2\Phi_2' + r\Lambda_2\cos\psi_2 = 0, \quad (6)$$

where  $\psi_1$  and  $\psi_2$  are defined by  $\psi_1 = \Phi_2(s - \Omega\tau) - \Phi_1(s) - \omega_2\tau - \Delta s$ ,  $\psi_2 = \Phi_1(s - \Omega\tau) - \Phi_2(s) - \omega_1\tau + \Delta s$ . In these equations  $\Lambda_m = \alpha\eta_m/\Omega$  is proportional to the mutual coupling strength,  $\xi_m = (1 + 2P_m)/\Omega T$  is the damping constant,  $r^2 = P_2/P_1$  is the ratio of the two pumps, and  $\Delta = (\omega_1 - \omega_2)/\Omega$  is the scaled detuning between the optical frequencies. Note that the terms multiplying  $\xi_m$  are  $\mathcal{O}(T^{-1/2})$  small and could be neglected. They are not needed for our bifurcation analysis of Eqs. (5)–(6), but are essential for all numerical studies of these equations by providing the natural damping term. Equations (5)–(6) have a simple interpretation when the delay  $\tau$  is neglected. Then the system reduces to two phase oscillators, one oscillating with  $\sigma_1 = 1$  ( $\sigma_m = 2\pi f_m/\Omega$ ) and the other with  $\sigma_2 = r$ , driven nonlinearly by the  $\cos(\Phi_1 - \Phi_2)$  term, their common phase difference.

Pertinent features of the bifurcation diagram of the rate equations [Fig. 3(c)] can be studied by analyzing slow time amplitude bifurcation equations valid for small  $\Lambda_m$ . For simplicity we shall restrict our analysis of the phase equations (5)–(6) to the case of small delays ( $\Omega\tau \ll 1$ ). The delay has the main effect of introducing external cavity modes into the system for sufficiently strong coupling, a regime we avoid by considering only weak coupling. A minor effect is to shift the bifurcation points, but it does not lead to new instabilities. For this case the leading approximation of the solution is given by:

$$\Phi_1 = A_1 \sin(s + \nu_1) + B_1, \quad (7)$$

$$\Phi_2 = A_2 \sin(rs + \nu_2) + B_2, \quad (8)$$

where  $A_m$  and  $B_m$  and  $\nu_m$  are slowly varying functions of  $s$ . They satisfy amplitude equations given by:

$$A_1' = -\xi_1 A_1/2 + r\Lambda_1 J_0(A_2)J_1(A_1) \sin(\Theta - \bar{\omega}\tau), \quad (9)$$

$$A_2' = -\xi_2 A_2/2 - (\Lambda_2/r)J_0(A_1)J_1(A_2) \sin(\Theta + \bar{\omega}\tau), \quad (10)$$

$$\Theta' = -\Lambda_1 F J_0(A_1)J_0(A_2), \quad (11)$$

where  $\bar{\omega} = (\omega_1 + \omega_2)/2$ ,  $\Theta = B_2 - B_1$ , and  $J_0$ ,  $J_1$  are Bessel functions and  $F = Cr^{-1}\cos(\Theta + \bar{\omega}\tau) - r\cos(\Theta - \bar{\omega}\tau)$ . From a linear stability analysis of the zero solution and assuming  $\bar{\omega}\tau = 2n\pi$ , we find a Hopf bifurcation point to a pure mode solution (only one of the free-running relaxation frequencies is undamped)  $A_1 \neq 0$ ,  $A_2 = 0$ , and  $\Theta_s = \pi/2$  located at:

$$\Lambda_1^{H1} = \xi_1/r. \quad (12)$$

At this point laser 1 oscillates strongly with  $\sigma_1 = 1$ . The solutions are  $\Phi_1 = A_1 \sin s + B_1$  and  $\Phi_2 = B_2$  in first approximation. A higher order analysis shows that  $\Phi_2 \cong (2r\Lambda_2)(r^2 - 1)^{-1}J_1(A_1) \sin \Theta \sin s + B_2$ , indicating that laser 2 oscillates with  $\sigma_1 = 1$  but smaller amplitude. We verify the analytically predicted location of the Hopf bifurcation point by integrating numerically Eqs. (5)–(6) for  $T = 1000$ ,  $\alpha = 10$ , and a small delay of  $\tau = 5$ . Figure 4 shows that both lasers undergo a Hopf bifurcation from steady state to a limit cycle at  $\Lambda_1 = 0.058$ , which agrees very well with the predicted value of  $\Lambda_1 = 0.055$ . Laser 1 oscillates with a much stronger amplitude than laser 2, clearly showing localized synchronization. The branches then evolve into a mixed solution where both relaxation oscillation frequencies are present. As we compare Fig. 4 to Fig. 3(c) we note the same sequence of bifurcation transitions. Thus the phase equations (5)–(6) are in good qualitative agreement with rate equations (1)–(4).

There exists a second Hopf bifurcation from the zero intensity solution to a pure mode solution  $A_1 = 0, A_2 \neq 0$ , and  $\Theta_s = -\pi/2$  at:

$$\Lambda_1^{H2} = \xi_2 r / C. \quad (13)$$

Both lasers now oscillate with frequency  $\sigma_2 = r$ . A critical value of the asymmetric coupling coefficient  $C^* = r^2$  determines which pure mode solutions will be the stable one. Specifically, if  $C < C^*$  we expect that laser 2 entrains to laser 1, and if  $C > C^*$  laser 1 entrains to laser 2. This explains the numerical observation of switching between the two possible localized states as  $C$  increases. Our analysis of the slow time equations (11)–(13) shows that two Hopf bifurcation points provide the mechanism for localized states characterized by dominant oscillations for one of the two lasers.

In conclusion, we have demonstrated experimentally, numerically, and analytically that localized synchronization is the main form of synchronization between two rela-

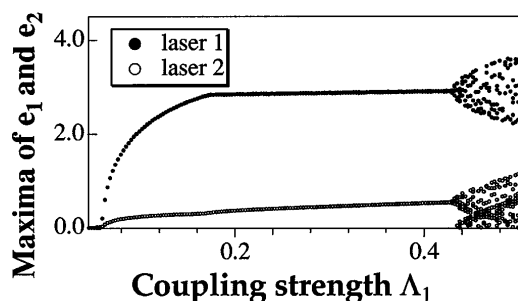


FIG. 4. Numerical bifurcation diagram computed with Eqs. (5)–(6) for  $T = 1000$ ,  $\tau = 5$ ,  $\alpha = 10$ ,  $P_1 = 0.313$ ,  $P_2 = 0.433$ ,  $C = 1.0$ , and  $\omega_1 = \omega_2$ . Both lasers undergo a Hopf bifurcation from steady state to a limit cycle at  $\Lambda_1 = 0.058$  very close to the analytically predicted of  $\Lambda_1^{H1} = 0.055$ . Laser 1 oscillates with a much larger amplitude than laser 2, clearly showing localized synchronization. The branches then become quasiperiodic at  $\Lambda_1 = 0.43$  as both relaxation oscillation frequencies are undamped.

tively different semiconductor lasers that are weakly coupled at a distance. One laser is forced to oscillate at the relaxation oscillation frequency of the other laser and with relatively smaller amplitude. In fact, synchronization may even appear in the form that the laser which is pumped at a higher level entrains to the laser which is pumped at a lower level. Physically, the relaxation oscillations can be undamped with a lower injection rate in the laser that is pumped at a lower level. Thus this laser will exhibit stronger amplitude oscillations and the strong oscillator will entrain the weak oscillator. The weak oscillator then in return injects the same oscillation frequency back into laser 1. The oscillation is self-initiated and self-sustained. These findings may have implications in large arrays of semiconductor lasers.

A.H. wishes to thank the NRC and AFOSR. T.E. was supported by U.S. AFOSR Grant AFOSR F49620-95-0065, NSF Grant DMS-9625843, NATO Grant 961113, the Fonds National de La Recherche Scientifique (Belgium), and the InterUniversity Attraction Pole of the Belgian government. The authors would like to thank R. Kalmus for technical assistance.

- [1] *Diode Laser Arrays*, edited by D. Botez and D.R. Scifres (Cambridge University Press, 1994).
- [2] C. Huygens, in *Oeuvres Complètes de Christiaan Huygens* (La Haye, Martinus Nijhoff, 1893), Vol. 5.
- [3] S.H. Strogatz and I. Stewart, *Sci. Am.* **269**, 102 (1993); S. Watanabe *et al.*, *Phys. Rev. Lett.* **74**, 379 (1995); I.R. Epstein and K. Showalter, *J. Phys. Chem.* **100**, 13 132 (1996).
- [4] V.V. Likhanskii and A.P. Napartovich, *Sov. Phys. Usp.* **33**, 242 (1990).
- [5] L. Fabiny *et al.*, *Phys. Rev. A* **47**, 4287 (1993).
- [6] R. Roy and K.S. Thornburg, *Phys. Rev. Lett.* **72**, 2009 (1994); K.S. Thornburg *et al.*, *Phys. Rev. E* **55**, 3865 (1997).
- [7] H.G. Winful and L. Rahman, *Phys. Rev. Lett.* **65**, 1575 (1990); H.G. Winful and S.S. Wang, *Appl. Phys. Lett.* **53**, 1894 (1988).
- [8] D.G. Aronson *et al.*, *Physica D* **41**, 403 (1990).
- [9] R.S. Mackay and S. Aubry, *Nonlinearity* **7**, 1623 (1994); D. Chen *et al.*, *Phys. Rev. Lett.* **77**, 4776 (1996).
- [10] R. Kuske and T. Erneux, *Zeitschrift für Angewandte Mathematik und Mechanik* **76**, 441 (1996).
- [11] R. Kuske and T. Erneux, *Opt. Commun.* **139**, 125 (1997).
- [12] T. Erneux, R. Kuske, and T.W. Carr, *SPIE* **2792**, 54 (1995).
- [13] G.C. Dente *et al.*, *IEEE J. Quantum Electron.* **26**, 1014 (1990).
- [14] D.J. Bossert *et al.*, in *Nonlinear Dynamics in Optical Systems Technical Digest (OSA)* **16**, 272 (1992).
- [15] T.B. Simpson *et al.*, *Phys. Rev. A* **51**, 4181 (1995).
- [16] R.A. Elliott *et al.*, *IEEE J. Quantum Electron.* **21**, 598 (1985); S.S. Wang and H.G. Winful, *Appl. Phys. Lett.* **52**, 1774 (1988).
- [17] T. Erneux *et al.*, *Phys. Rev. A* **53**, 4372 (1996); P. Alsing *et al.*, *Phys. Rev. A* **53**, 4429 (1996).